RESEARCH ARTICLE

High-power and short-duration ablation with the Qdot+ algorithm for pulmonary vein isolation and the right superior ganglion plexus ablation without fluoroscopy

Edward Koźluk[1] (iD)**, Agnieszka Piątkowska[2,1]** (iD)**, Dariusz Rodkiewicz[1]** (iD)**,**

Grzegorz Opolski[1] (iD)

[1] I Chair and Department of Cardiology Medical University of Warsaw, Warsaw, Poland
[2] Department and Clinic of Emergency Medicine, Wrocław Medical University, Wrocław, Poland
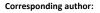
Abstract

In this report we present pulmonary vein and posterior box isolation together with the right superior ganglion plexus ablation using the Qdot Micro catheter without fluoroscopy. We describe different possibilities of this new technology for catheter ablation. The main advantages of this catheter to potentially increase ablation safety and effectiveness are discussed. Specifically, the possibility to perform high-density mapping with the lowest available distance between points. Furthermore, the possibility to decrease the risk of collateral tissue damage and to improve atrial linear lesions contiguity, transmurality and durability due to the dominance of resistive heating supported by the feedback temperature control. Finally, the possibility to shorten the procedure and fluoroscopy duration due to the high shortening of application duration to 4 seconds only.

Keywords: atrial fibrillation · pulmonary vein isolation · high power short duration ablation · Qdot Micro catheter · ganglion plexi ablation · zero-fluoroscopy ablation

Corresponding author:

Dariusz Rodkiewicz, I Chair and Department of Cardiology, Medical University of Warsaw, Poland
e-mail: elektrofizjologia@wum.edu.pl

Introduction

Isolation of the pulmonary veins is the most effective treatment for atrial fibrillation (AF)[1]. The reference method of this procedure is radiofrequency (RF) ablation with a single-point catheter using an electroanatomical system. Its main limitations are the long duration of the procedure and still unsatisfactory effectiveness [2]. Hence, methods are sought to increase its effectiveness and safety, combined with shortening of the procedure's duration. One of the ways is to use single-shot devices such as balloons or the pulmonary vein ablation catheter [2-3]. An alternative is to shorten the time of a single application. In part, it was possible to achieve this by controlling the pressure of the electrode against the tissue, especially in combination with the so-called "close" protocol [4]. The next big step seems to be increasing the power to 90W, which allows to shorten a single application to 3-4 seconds. The primary aim of this article is to present the new Qdot catheter, which is the first device to enable this procedure [5].

In recent years, there has been an increased interest in cardioneuroablation [6-10]. A beneficial effect has been demonstrated by this type of procedure for patients with reflex syncope [6-10]. Since in some patients with sinus node disease the syncope is functional (patients with rapid rhythm-induced pauses, drug-induced sinus node disease, athletes with bradycardia) [11], ablation of the parasympathetic ganglia is often effective for them and allows them to avoid pacemaker implantation [6, 12]. To the best to our knowledge, there have been no studies presenting cardioneuroablation using high-power short-duration ablation. Thus, our second aim is to present the first experience with Qdot+ protocol in pulmonary vein ablation together with cardioneuroablation.

Case presentation

To illustrate these aims, we present the case of a 77-year-old female after the right atrial inferior isthmus ablation because of typical atrial flutter 5 years ago. For about 2 years the patient experienced paroxysmal AF with EHRA score III [1]. The symptoms of arrhythmia consisted of palpitations, chest discomfort, shortness of breath, headache and dizziness. Concealed sinus node dis-

ease was also diagnosed (during treatment with a beta-adrenolitics an episode of syncope occurred and in 24-hour ECG holter monitoring there were pauses of automatism up to 4 seconds). These symptoms resolved after the discontinuation of antiarrhythmic drugs. The patient reported an episode of gastrointestinal bleeding. Since pharmacotherapy was not possible, the patient was qualified for pulmonary vein isolation together with parasympathetic ganglion plexi ablation. Before the procedure, thromboembolic material in the left atrium was excluded using transesophageal echo. Patent foramen ovale (PFO) was diagnosed with small interatrial leak. Because the transseptal puncture was not necessary, the patient was qualified for ablation without fluoroscopy using the technique we previously described [13].

At the beginning of the procedure the patient was on AF. The catheters were introduced into the coronary sinus and the right ventricle under the control of CARTO system. Using the Qdot catheter, long transseptal sheaths were introduced via the right femoral vein into the superior vena cava. The right atrial voltage map was made using the LassoNav catheter. On its basis, a Qdot catheter was introduced into the left atrium through the PFO. Over this catheter two transseptal sheaths were successively inserted into the left atrium. A map of the left atrium and proximal parts of the pulmonary veins was obtained using the CARTO system. The pulmonary vein potentials were diagnosed in all four pulmonary veins. With the use of the Qdot+ algorithm (90W for 4 s), all pulmonary vein isolation was performed according to the "close" protocol, verified with the LassoNav catheter (Fig. 1-3).
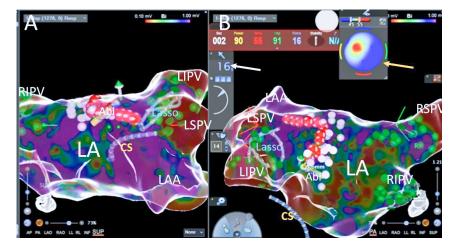

Fig. 1. One of the RF aplications during left pulmonary veins isolation; ressure (the white arrow) of the catheter on the posterior wall is 16g. Bulls' eye (the yellow arrow) indicate good pararell contact of the catheter tip with the left atrial tissue with optimal temperature increase at the second second of aplication (red zone in left superior quadrant); green dots – pulmonary vein potentials, pink dots – fragmented potentials, red dots – ablation points; Abl – ablation catheter, CS – catheter in the coronary sinus, LA – the left atrium, LAA – the left atrial appandage, Lasso – LassoNav catheter inside the left inferior pulmonary vein, LIPV – the left inferior pulmonary vein, LSPV – the left superior pulmonary vein, RIPV – the right inferior pulmonary vein, RSPV – the right superior pulmonary vein; panel A – superior view, panel B – posteriori view on the left atrium

At the beginning of the left superior pulmonary vein isolation, the sinus rhythm returned without pathological pause. After pulmonary veins' isolation the right superior ganglion plexus was mapped using 100 ms cycle length stimulation (mixed type reactions were observed). The pacing induced unsustained atypical atrial flutter. Ablation was performed at ganglionated plexi (GB) stimulation sites, however we did not observe significant acceleration of the sinus rhythm. Because of the small distance between the lines, the posterior segment was isolated (the line in the roof and in the lower part of the posterior wall) (Fig. 4-5). LassoNav catheter mapping was performed with accessory applications to obtain full pulmonary veins and the posterior segment isolation. The post- procedure and follow-up (on the following day) transthoracic echocardiography did not reveal any fluid in the pericardium.

Duration of the procedure was 140 min (puncture and catheter introduction 20 min, right atrial mapping – 10 min, transseptal access – 10 min, left atrial and pulmonary vein mapping – 20 min, left pulmonary vein isolation – 22 min, right pulmonary vein isolation – 33 min, mapping of the right superior GP and its ablatio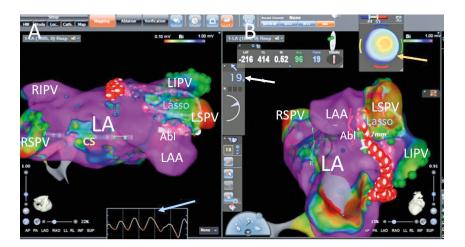n – 10 min, posterior segment isolation –10 min, control mapping of the pulmonary veins and posterior wall – 5 min). The procedure was performed without the use of fluoroscopy. The total time of 203 RF current applications was 13 min 32 s. After the procedure we observed sinus rhythm 75 bpm, BP 115/70 mmHg. There were no complications. Sinus rhythm was maintained during the postoperative monitoring. On the next day, the patient was discharged home in good general condition. Pharmacotherapy with dabigatran, rosuvastatin and a proton pump inhibitor was maintained. There were no palpitations or syncope during follow-up.

Fig. 2. Another RF aplications on the limbus between the left atrial appandage and the left superior pulmonary vein' pressure (the white arrow) of the catheter on the limbus is 19g. Bulls' eye (the yellow arrow) indicate good perpendicular contact of the catheter tip with the left atrial tissue with optimal temperaturę increase at the fourth second of aplication (red zone in central part); green dots – pulmonary vein potentials, red dots – ablation points; blue arrow – respiratory curve; Abl – ablation catheter, CS – catheter in the coronary sinus, LA – the left atrium, LAA – the left atrial appandage, Lasso – LassoNav catheter inside the left superior pulmonary vein, LIPV – the left inferior pulmonary vein, LSPV – the left superior pulmonary vein, RIPV – the right inferior pulmonary vein, RSPV – the right superior pulmonary vein; panel A – superior view, panel B – modyfied left anterior oblique view on the left atrium
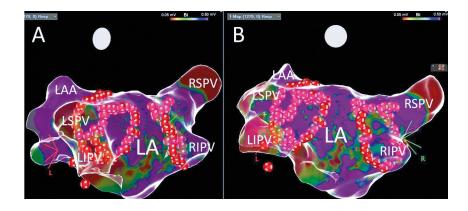

Fig. 3. The LAO projection (panel A) and posteriori view (panel B) on the left atrium after pulmonary vein isolation; red dots – ablation points; LA – the left atrium, LAA – the left atrial appandage, LIPV – the left inferior pulmonary vein, LSPV – the left superior pulmonary vein, RIPV – the right inferior pulmonary vein, RSPV – the right superior pulmonary vein

Discussion

The Qdot micro catheter is a new generation catheter that offers advantages of the recent technological developments. Below we present all advantages of this catheter.

Typical thermocool catheter with pressure control

The design of the Qdot Micro catheter allows it to be used as a typical ablation catheter with a cooled tip and with

pressure control. This is similar to the newest version of Thermocool Smart-touch SF catheter (used at present in centers not involved in the implementation program for the Qdot Micro catheter), employing a porous irrigation tip with the same contact force sensor to provide directional contact force information. This makes it possible to calculate the "ablation index", parameters which together with the "close protocol " increased the success rate and decreased the complication risk during left atrial ablations in recent years. This catheter may be used in two options: unidirectional and bi-directional with different curves (the second one is preferred in our center). This catheter also allows temperature measurement, however this will be discussed below. Therefore, the new Qdot Micro catheter can be used with the same mode as the Thermocool Smarttouch SF catheter.
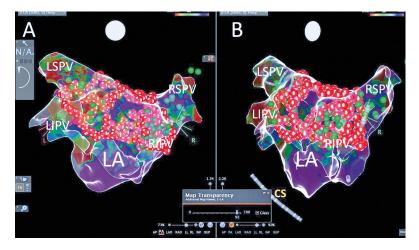

Fig. 4. The final bipolar voltage map after isolation of the pulmonary veins and posterior wall in PA projection (panel A) and the right posteriori oblique view (panel B); green dots – pulmonary vein potentials before ablation, red dots – ablation points; CS – decapolar catheter in the coronary sinus, LA – the left atrium, LIPV – the left inferior pulmonary vein, LSPV – the left superior pulmonary vein, RIPV – the right inferior pulmonary vein, RSPV – the right superior pulmonary vein

High-density mapping

High density mapping is one of the milestones of modern electrophysiology. It allows to increase the precision of arrhythmogenic substrate mapping and thus increase the success rate in complex arrhythmias [14]. There are different technical solutions for high density mapping. The resolution of this mapping varies with catheters from different brands. For example, the Orion catheter (Boston Scientific) is fold-out rosette consisting of 8 arms. There are 8 small electrodes with an area of 0.4 mm^2 spaced 2.5 mm apart (a total of 64 electrodes) on each arm. The electrode is compatible with the Rhythmia system (Boston Scientific) and enables automatic map-making from high density of points (annotation of signals is automatic as it would be impossible to conduct manually). Another example is the Advisor HD-grid (Abbot) high-density mapping catheter co-operating with the EnSite system (Abbott) consisting of 4 electrode strands (1 mm length/width; 3 mm apart) with 4 electrodes each. The distance between the electrodes in both directions is the same, thanks to what we obtain 24 pairs of electrodes for bipolar recordings and 16 electrodes for unipolar recordings). Due to the even distribution, it is possible to evaluate bipolar electrographs in both perpendicular planes. Another example of catheter for high density mapping is the Octarey catheter (Johnson & Johnson) cooperating with CARTO 3 system. This catheter consists of 8 diverging flexible arms containing 6 small electrodes (0.5 mm long) 2 mm apart (48 electrodes in total). Unlike the Qdot micro catheter, all of the above are only mapping catheters and require a separate ablation catheter.
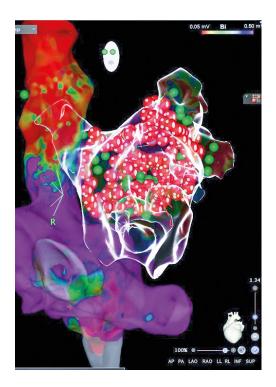

Fig. 5. Bipolar voltage map of the right atrium, on the basis of which the transseptal sheats with catheters were introduced into the left atrium via PFO together with the final left atrial anatomical glass map after pulmonary vein isolation and posterior segment isolation; LAO projection

In the Qdot micro catheter three microelectrodes are placed 1,5 mm apart around the distal end of the ablation tip (Fig. 6). The size of the electrodes is 0,32 mm in diameter with a surface area of 0,086 mm^2 each. Currently, these
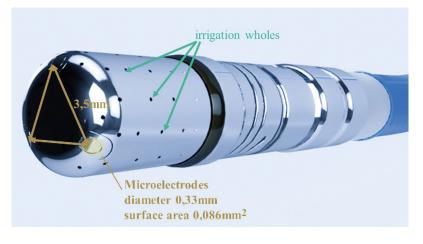
Fig. 6. Tip of the Qdot catheter; the microelectrodes are placed one and a half millimeters apart around the distal end of the ablation tip; the size of the electrodes is point three three millimeters in diameter with a surface area of point zero eight six millimeters each; the small surface area of the microelectrodes enables discrete, high resolution signals with less far-field information than the larger ablation tip affords

Fig. 7. The skeleton of the Qdot Micro™ Catheter tip presents channels within the wall of the tip itself, into which the thermocouples and microelectrodes are placed; as mentioned in the main text this designe places the thermocouples in close proximity to the tip--tissue interface, enabling temperature to be measured as the tissue is heated by the application of radiofrequency energy; A – thicker wall accomodates channels, B – thermocouple channels, C – microelectrode channels

are the smallest microelectrodes and the closest spacing between them among the available high-density mapping catheters. The small surface area of the microelectrodes enables discrete, high-resolution signals with less farfield information than the larger ablation tip affords. The microelectrode signals can be displayed as unipolar and bipolar electrograms. The highest voltage electrogram among three microelectrode pairs is used to apply color to the voltage map. The microelectrodes signals do not apply to LAT (local activation time) maps. The bipolar electrograms are displayed as microelectrode pairs: 1-2, 2-3, 3-1. The numbers of the microelectrodes may be displayed on the CARTO 3 map, which can help with the selection of microelectrodes pairs for pacing. Microelectrode pacing may facilitate very local capture and is routed between microelectrode pairs. Pacing is not routed between any microelectrode and a standard electrode. Microelectrodes are more sensitive to power line noise during the RF application than the larger electrodes. The CARTO 3 system employs advanced power line noise filters for exceptional signal quality. This could lead to damage of monitoring during RF current application. When using the Confidense module with continuous mapping feature, the stability filter must be used to prevent acquisition of points during catheter motion.

High density temperature control (including catheter orientation)

The predecessor catheter Smarttouch SF employs a single thermocouple in the center of the ablation tip, surrounded by cooling saline. Using this design, the temperature should be monitored only to confirm that the irrigation is adequate (and temperature rise during ablation may indicate blocked irrigation). In the Qdot catheter there are 6 thermocouples placed in the channels within the wall of the distal electrode itself around this electrode in close proximity to the tissue interface (Fig. 7). Three thermocouples are located distally around the catheter tip (0,075 mm from the real tip), and three thermocouples are located proximally around the catheter tip (3 mm from the real tip) (Fig. 6-7). The CARTO 3 system displays the temperature measured on the catheter, which helps to confirm energy delivery to the tissue and the tip-tissue contact stability (Fig. 1-2). The temperature color display aids in understanding the orientation of the catheter tip to the tissue during RF ablation(-Fig. 1-2). Red color centered on the "bulls' eye" indicates that the catheter is touching the tissue in perpendicular orientation (Fig. 2). Red color on one side of the display indicates heating on that side of the ablation tip, which signals that the ablation tip is connecting the tissue in a parallel orientation (Fig. 1).

Feedback temperature control

It has been shown that an increase of temperature >85°C is an important risk factor for the so-calle steam pop, which may be the cause of cardiac tamponade [15]. To increase the safety of the RF application, the temperature is measured every 33 ms and if it increases above programmed

value then the power is reduced or saline flow is increased [15]. There are two different modes of feedback control (Fig. 8-9).

When the maximum power of RF current is set for lower or equal 35 W, after activation of the generator, irrigation begins at four milliliters per minute for the pre-determined RF delay period (few seconds). After the onset of RF energy delivery, we begin to see a temperature rise. In this instance the temperature rise is steep and a burst of the higher flow rate (15 mL/min) is automatically applied. When the temperature drops, the irrigation is returned to the lower flow rate (4 mL/min). As the temperature reaches the target (65°C is recommended) there is another burst of the higher irrigation flow rate, until the temperature drops below the target. If the temperature exceeds the target temperature, another burst of the higher flow rate is applied, as well as decrease in the power delivered. When the temperature drops, the power increases again, and the flow rate decreases to the lower rate (Fig. 8).

When the maximum power of RF current is set for > 35 W, the irrigation flow rate starts at 15 mL/min. If the measured temperature does not rise, the irrigation rate drops to 4 mL/min until the temperature exceeds the preset max low flow temperature value. Once the temperature rises above this temperature, the irrigation rate is increased to 15 mL/min. The irrigation rate and the power are automatically adjusted to maintain the temperature between the max low flow and the target value, and the primary means of temperature control is the irrigation flow rate. Power is adjusted if the higher irrigation rate is insufficient to affect a temperature response. If the temperature reaches the predetermined cut-off temperature level, the RF application will be automatically terminated (Fig. 9).
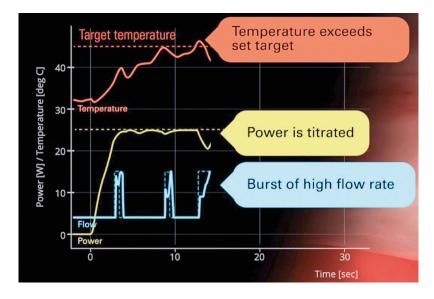

Fig. 8. Feedback temperature control when the maximum power of RF current is set for lower or equal 35W; description in the main text
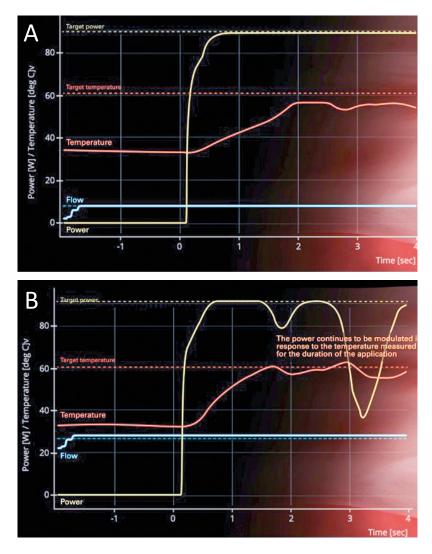

Fig. 9. Feedback temperature control when the maximum power of RF current is set for lower or equal 35W; description in the main text; panel A – temperature do not reach target level, panel B – temperature reach target level

High power, short duration ablation

The greatest advantage of the Qdot catheter is the ability to perform a high-energy short duration ablation [15-17, 19]. In RF ablation, the tissue damage occurs in two consecutive phases. The first is resistive phase, the second is the conductive phase. The first one depends directly on the amount of energy delivered at the catheter-tissue interface. The second one is mainly contingent on the time of application and results from the gradual passive heating extend to deeper tissue layers. When the temperature reaches 50ºC, an irreversible myocardial tissue injury occurs. At lower temperatures, the reversible damage often occurs with accompanying tissue edema [15]. In traditional RF ablations, the second effect dominates. It is difficult to predict when the application is transmural. There is a risk of underheating, which may be masked by the tissue edema (hence the acute effect may be effective and after the edema disappearance, conduction or automatism recurs). Alternatively, the overheating causes damage to neighboring organs. Hence, in order to increase the safety and effectiveness of the radiofrequency current ablation, the concept of high-power short-duration applications was developed [15-17, 19]. When using high power for a few seconds, we observe only the resistive effect. In animal experiments, it was shown that the best efficacy and safety rates was obtained with applications duration of 4 seconds [15-17]. Using the power of 90 W at this duration, the depth of lesion was 3,6+0,6 mm and the width was 10,4 + 1,2 mm [15]. The variances of these parameters were smaller than after classical applications, which resulted in more frequent continuous lines without the gap both in direct [15-17] observation and after 30 days follow-up [16]. As the thickness of the atrium muscle is comparable to the depth of the lesion [18], no damage to the adjacent organs was also observed [15].

The tissue overheating may result in steam pop which can cause cardiac tamponade. The steam pop was observed in animal models if temperature of the catheter-tissue interface was > 85˚C or the catheter pressure was > 40g [15]. To avoid this phenomenon, a feedback temperature control was introduced. Without this protection, the phenomenon of steam pop was noticed during 3/174 applications (1,7%). After the introduction of this algorithm, this phenomenon was not observed during 233 applications. Shortening the time of a single application during the isolation of the right superior pulmonary vein resulted in a reduction in their duration compared to classic procedures in animal studies from 270 +60 s to 33 + 6 s [15].

Qdot procedure in our patient

There is limited experience with PVI isolation using Qdot catheter and high-power and short duration ablation. A single clinical study assessed its feasibility, safety and short-term effectiveness on 52 patients [19]. Direct isolation was achieved for all pulmonary veins including an adenosine/isoproterenol check. The study showed favorable mean procedure and fluoroscopy duration compared to classic ablation. There were 2 complications: a pseudoaneurysm and an asymptomatic cerebral thromboembolism. After 3 months of follow-up, 49 patients (94,2%) had sinus rhythm, whereas 2 had AF and one had atrial flutter. To the best of our knowledge, there is no data about GP ablation using high-power short duration applications. However, all the preclinical data suggest that when using this form of ablation, the damage is transmural. Thus, it should be effective in this kind of ablation.

Conclusion

The Qdot Micro catheter presented in this article offers some new advantages potentially increasing ablation safety and effectiveness. Specifically, the possibility to perform high-density mapping with the lowest available distance between points. Furthermore, the possibility to decrease the risk of collateral tissue damage and to improve atrial linear lesions contiguity, transmurality and durability due to the dominance of resistive heating supported by the feedback temperature control. Finally, the possibility to shorten the procedure and fluoroscopy duration due to the high shortening of application duration to 4 seconds only.

References

1. Hindricks G, Potpara T, Dagres N, Arbelo E, Bax JJ, Blomström-Lundqvist C, et al. 2020 ESC Guidelines for the diagnosis and management of atrial fibrillation developed in collaboration with the European Association for Cardio-Thoracic Surgery (EACTS). Eur Heart J [Internet]. 2021 Feb 1;42(5):373–498. Available from: https://academic.oup.com/eurheartj/article/42/5/373/5899003
2. Koźluk E, Balsam P, Peller M, Kiliszek M, Lodziński P, Piątkowska A, et al. Efficacy of multi-electrode duty-cycled radiofrequency ablation in patients with paroxysmal and persistent atrial fibrillation. Cardiol J [Internet]. 2013 Dec 11;20(6):618–25. Available from: http://czasopisma.viamedica.pl/cj/article/view/36496

3. Koźluk E, Gaj S, Piątkowska A, Kiliszek M, Lodziński P, Dąbrowski P, et al. Evaluation of safety and the success rate of cryoballoon ablation of the pulmonary vein ostia in patients with atrial fibrillation: A preliminary report. Kardiol Pol [Internet]. 2010;68(2):175–80. Available from: https://www.mp.pl/kardiologiapolska/en/node/9682/pdf

4. Phlips T, Taghji P, El Haddad M, Wolf M, Knecht S, Vandekerckhove Y, et al. Improving procedural and one-year outcome after contact force-guided pulmonary vein isolation: the role of interlesion distance, ablation index, and contact force variability in the 'CLOSE'-protocol. EP Eur [Internet]. 2018 Nov 1;20(FI_3):f419–27. Available from: https://academic.oup.com/europace/article/20/FI_3/f419/4791151

5. Reddy VY, Grimaldi M, De Potter T, Vijgen JM, Bulava A, Duytschaever MF, et al. Pulmonary vein isolation with very high power, short duration, temperature-controlled lesions. JACC Clin Electrophysiol [Internet]. 2019 Jul;5(7):778–86. Available from: https://linkinghub.elsevier.com/retrieve/pii/S2405500X19303032

6. Pachon M JC, Pachon M EI, Pachon M JC, Lobo TJ, Pachon MZ, Vargas RNA, et al. "Cardioneuroablation" – new treatment for neurocardiogenic syncope, functional AV block and sinus dysfunction using catheter RF-ablation. EP Eur [Internet]. 2005 Jan 1;7(1):1–13. Available from: https://academic.oup.com/europace/article/7/1/1/432294

7. Pachon M JC, Pachon M EI. Differential effects of ganglionic plexi ablation in a patient with neurally mediated syncope and intermittent atrioventricular block: a commentary. EP Eur [Internet]. 2017 Jan 1;19(1):1–3. Available from: https://doi.org/10.1093/europace/euw133

8. Yao Y, Shi R, Wong T, Zheng L, Chen W, Yang L, et al. Endocardial autonomic denervation of the left atrium to treat vasovagal syncope. Circ Arrhythmia Electrophysiol [Internet]. 2012 Apr;5(2):279–86. Available from: https://www.ahajournals.org/doi/10.1161/CIRCEP.111.966465

9. Piotrowski R, Baran J, Kułakowski P. Cardioneuroablation using an anatomical approach: a new and promising method for the treatment of cardioinhibitory neurocardiogenic syncope. Kardiol Pol [Internet]. 2018 Dec 17;76(12):1736–8. Available from: https://journals.viamedica.pl/kardiologia_polska/article/view/83108

10. Koźluk E, Piątkowska A, Rodkiewicz D, Kowalczuk N, Opolski G. Kardioneuroablacja w omdleniach odruchowych — nowa nadzieja dla trudnych pacjentów [in Polish]. Forum Med Rodz [Internet]. 2019;13(5):223–31. Available from: https://journals.viamedica.pl/forum_medycyny_rodzinnej/article/view/65347

11. Adán V, Crown LA. Diagnosis and treatment of sick sinus syndrome. Am Fam Physician [Internet]. 2003 Apr 15;67(8):1725–32. Available from: http://www.ncbi.nlm.nih.gov/pubmed/12725451

12. Chen Y-W, Bai R, Lin TAO, Salim M, Sang C-H, Long D-Y, et al. Pacing or ablation: which is better for paroxysmal atrial fibrillation-related tachycardia-bradycardia syndrome? Pacing Clin Electrophysiol [Internet]. 2014 Apr 1;37(4):403–11. Available from: https://doi.org/10.1111/pace.12340

13. Koźluk E, Łojewska K, Hiczkiewicz J. First experience with left atrial arrhythmia ablation using a bidirectional steerable transseptal sheath (Vizigo) visible in the CARTO system as a method to reduce fluoroscopy. Eur J Transl Clin Med [Internet]. 2020;3(2):18–21. Available from: http://dx.doi.org/10.31373/ejtcm/131049

14. Kodali S, Santangeli P. How, when, and why: high-density mapping of atrial fibrillation. Card Electrophysiol Clin [Internet]. 2020 Jun;12(2):155–65. Available from: https://linkinghub.elsevier.com/retrieve/pii/S1877918220300186

15. Leshem E, Zilberman I, Tschabrunn CM, Barkagan M, Contreras-Valdes FM, Govari A, et al. High-power and short-duration ablation for pulmonary vein isolation. JACC Clin Electrophysiol [Internet]. 2018 Apr;4(4):467–79. Available from: https://linkinghub.elsevier.com/retrieve/pii/S2405500X17311726

16. Barkagan M, Contreras-Valdes FM, Leshem E, Buxton AE, Nakagawa H, Anter E. High-power and short-duration ablation for pulmonary vein isolation: Safety, efficacy, and long-term durability. J Cardiovasc Electrophysiol [Internet]. 2018 Sep 20;29(9):1287–96. Available from: https://onlinelibrary.wiley.com/doi/abs/10.1111/jce.13651

17. Takigawa M, Kitamura T, Martin CA, Fuimaono K, Datta K, Joshi H, et al. Temperature- and flow-controlled ablation/very-high-power short-duration ablation vs conventional power-controlled ablation: Comparison of focal and linear lesion characteristics. Hear Rhythm [Internet]. 2021 Apr;18(4):553–61. Available from: https://linkinghub.elsevier.com/retrieve/pii/S1547527120310328

18. Cabrera JA, Ho SY, Climent V, Sanchez-Quintana D. The architecture of the left lateral atrial wall: a particular anatomic region with implications for ablation of atrial fibrillation. Eur Heart J [Internet]. 2008 Jan 17;29(3):356–62. Available from: https://academic.oup.com/eurheartj/article-lookup/doi/10.1093/eurheartj/ehm606

19. Glashan CA, Tofig BJ, Tao Q, Blom SA, Jongbloed MRM, Nielsen JC, et al. Multisize Electrodes for Substrate Identification in Ischemic Cardiomyopathy. JACC Clin Electrophysiol [Internet]. 2019 Oct;5(10):1130–40. Available from: https://linkinghub.elsevier.com/retrieve/pii/S2405500X19304128